Estimation of water layer correction in shallow time-lapse streamer data sets

Beng S. Ong, Jeshurun Hembd, CGG and Arjun Srinivasan, Dez Chu, David H. Johnston, Exxon Mobil Corporation

Summary

Time-lapse seismic surveys are intended to measure changes in the subsurface related to reservoir production. Accurate estimation of the reservoir level requires corrections to layers above the reservoir, including the water layer. Water layer changes can be attributed to ocean tides and water velocity changes, which require offset- and depth-dependent timing corrections. These can be difficult to estimate in shallow water marine streamer data sets; thus, we developed a completely data-driven method that reduces timing differences and is effective in both shallow and deep water.

Introduction

In time-lapse data, the aim is to detect changes in the subsurface related to production in the reservoir. These area of interest in time-lapse marine data are generally below the water bottom. However, the water layer itself changes between acquisitions. This affects the wavefield propagation of reflections from all interesting subsurface events.

In towed streamer data sets, the effects of water layer changes are immediately apparent on time-shift maps. The time shifts appear as stripes parallel to the sailing direction. These time shifts propagate down through the data, and can be significant enough to obscure important changes near the reservoir.

Changes in the water layer can be classified into two main types: water velocity variation and changes in the water depth due to tides. Both types introduce timing differences to all subsurface reflections that vary with reflector depth and recording offsets. A water velocity change will introduce a time shift that increases with offset, while a water depth change produces the opposite effect.

Different methods have been used to invert for tidal and velocity changes in time-lapse data. One way is to introduce external information such as tidal maps, differential GPS (Henry, 2004), and the direct measurement of water velocity for the correction (Lacombe, 2006). Another method uses an equation proposed by Landrø and Stammeijer (2004) applied to the water layer (Lacombe, personal communication, 2013). Then, it relates the time-shift measured at the water bottom to 1D travel-time change due to tide and water velocity changes. However, this method relies solely on measuring timing differences at the water bottom and hence does not work well in shallow water because of limited near offset data and often poorly recorded water bottom.

We extended the method by Lacombe to a more general case that allows reflectors below the water bottom to be used for time-shift measurements. Our method is completely data-driven and thus reliable for both shallow- and deep-water surveys without requiring external information. Using reflectors other than the water bottom not only resolves the shallow water issue, but it also stabilizes the inversion by allowing multiple windows. We chose reflectors above the reservoir where no significant time-lapse effects were expected so that overburden changes between water layer and reservoir can be neglected.

Theory

The measured time-shift of a reflector, $\Delta t(x)$, between the monitor and baseline data sets that both have normal move-out (NMO) applied using baseline velocity, for offset x is defined as

$$\Delta t(x) \coloneqq t_M(x) - t_B(x) \qquad (1)$$

where $t_M(x)$ and $t_B(x)$ are the baseline velocity NMO-travel times for the same reflector in the monitor and baseline data sets, respectively. We assume the baseline velocity is accurate and produces flat gathers for the same image point; hence, $t \coloneqq t_B(x)$ for all offsets x.

The change in water velocity, dv, and water depth, dz, introduces a zero offset travel-time difference between the monitor and the baseline

$$dt \approx t_0\left(\frac{dz}{z_0} - \frac{dv}{v_0}\right) \qquad (2)$$

where v_0 is the water velocity of the baseline survey, and t_0 is the baseline zero offset two-way time of water bottom.

Landrø and Stammeijer's equation used by Lacombe (personal communications, 2013) applied within the water layer is given by

$$\Delta t(x) = dt - \frac{dv}{t_0 v_0^3} x^2 \qquad (A)$$

We denote the root-mean-square (RMS) velocity of the baseline and monitor to be v_{rms} and $v_{M,rms}$, respectively. We assume the only difference between the two velocities is due to the water layer: water velocity, dv, and depth, dz. The baseline velocity, also referred to as reference velocity, is known, while the monitor velocity is not.

To derive the extended equation, we start with 1D travel-time for monitor survey NMO with the reference velocity

$$t_M^2(x) = l^2 + \left(\frac{x}{v_{M,rms}}\right)^2 - \left(\frac{x}{v_{rms}}\right)^2 \qquad (3)$$

where l is the monitor survey zero offset two-way time for a reflector. From Equation 2, we can rewrite l as $l = t + dt$.

DOI http://dx.doi.org/10.1190/segam2015-5866701.1

The extended equation relating measured time-shift at any reflectors to tidal and water velocity change is

$$\Delta t(x) = dt - \frac{t_0}{t^2}\left[\alpha\frac{dv}{v_0} + \beta\frac{dz}{z_0} + \gamma\right]x^2 \qquad \text{(B)}$$

$$\alpha = \frac{v_0^2 + v_{rms}^2(t)}{2v_{rms}^4(l)} \qquad \text{(i)}$$

$$\beta = \frac{v_0^2 - v_{rms}^2(t)}{2v_{rms}^4(l)} \qquad \text{(ii)}$$

$$\gamma = \frac{v_{rms}^2(t) - v_{rms}^2(l)}{2v_{rms}^4(l)} \qquad \text{(iii)}$$

In effect, the alpha term accounts for bulk dv and dz correction, while the beta term is an additional correction for reflectors below water bottom. The gamma term accounts for velocity variation between layers.

The beta term (Equation ii) is zero when the reflector used is the water bottom, and gamma (Equation iii) is essentially zero for a slowly varying velocity. When both conditions are true, Equation B reduces to Equation A.

For each offset, x, we obtain a measured time-shift, $\Delta t(x)$ for a reflector. Then, we fit a curve of the form: $y = c + ax^2$. The intercept c is dt; thus, coefficients (Equations i-iii) can be computed because the baseline velocity is known. This leads to two linear equations with two unknowns: dv and dz.

Once we have dv and dz, we can obtain $v_{M,rms}$ from v_{rms} by replacing the water velocity with $v + dv$ and adjusting the water bottom time to $t_0 + dt$ (in interval velocity domain). Next, we can remove the timing differences caused by water layer variations from the monitor survey by first applying NMO correction with $v_{M,rms}$ on non-NMO data and then removing the zero-offset time difference, dt. Finally, we reverse the NMO correction using the reference velocity.

Synthetic Simulation

To verify the accuracy of our method, we used a synthetic data set with a two-layer model. The first layer was water, and the second layer had a velocity of 2000 m/s. For our baseline data, the water depth was 150 m, and the water velocity was 1500 m/s. Hence, the baseline water bottom travel-time was 200 ms. For this synthetic experiment, we used $dv = 30\ m/s$ and $dz = 6m$ resulting in $dt \approx 4\ ms$.

A set of baseline and monitor data were generated for the same common depth point (CDP), and NMO was applied using the reference velocity. In this experiment, we had a water bottom at t = 200 ms and a deeper reflector at t = 400 ms in each set of gathers. We measured the time-shift between the baseline and monitor data for the deeper reflector.

First, we evaluated the accuracy of these equations in predicting the time-shift with the exact dv and dz for a reflector at t = 400 ms by comparing it to the measured time-shift.

Equation A gave the poorest fit to the measured time-shift, while Equation B gave a very accurate fit. All three terms (Equations i-iii) in Equation B were essentials for accurately predicting time-shifts (Figure 1).

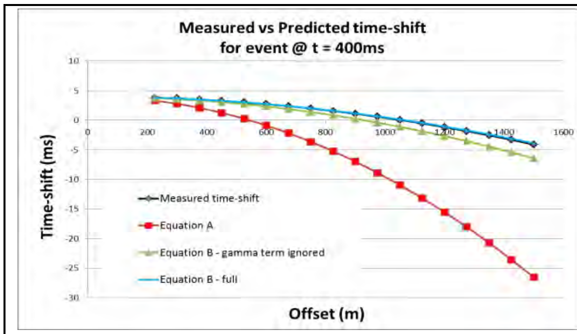

Figure 1: The black line is the measured time-shift from the synthetic data. The red line is Equation A and differs significantly from the black line. The difference increases as offset increases. The green line is Equation B without the gamma term and is much closer to the measured points. The blue line is the full Equation B and agrees very well with the measured data points.

Next, we used the measured time-shift along with Equations A and B to estimate dv and dz. In our synthetic example, we had 48 offsets for each CDP ranging from 225 to 3750 with 75 m increments. However, because not all offsets can be used in field data due to noise, NMO stretch, and imperfect velocity, we purposely used only a small subset of the synthetic data to invert (Figure 2).

Deeper Layer	Equation A		Equation B	
Event @ t = 400 ms	dv (m/s)	dz (m)	dv (m/s)	dz (m)
Using first 3 offsets	2.7	3.27	29.68	5.97
Using first 18 offsets	2.7	3.28	29.69	5.98

Figure 2: The exact dv and dz are 30 and 6, respectively. Equation B gives a much more accurate estimate than Equation A.

Field Data

Next, we applied our method to a data set obtained from the Zafiro field in Equatorial Guinea. In this survey, the two-way water bottom time ranged from 80 ms to 1400 ms, and the water depth was between 67 m and 1000 m. The large variation in water depth allowed us to evaluate the effectiveness of the method for both shallow and deep water. The smallest offset class was 225 m.

 DOI http://dx.doi.org/10.1190/segam2015-5866701.1

This data underwent de-multiple process, receiver motion correction, and 3D water column statics (WCS) correction. The WCS used the individual vintage only to correct the discontinuity between adjacent sail lines. To measure the time shift between the monitor and baseline, we co-binned the traces. Then, dv and dz corrections were applied in the sail-line domain.

We used multiple windows, all below the water bottom but above reservoir, for the time-shift measurement, and dv and dz were inverted through Equation B.

For comparison, we also applied Equation A to the data separately. The time-shift was measured at the water bottom, and dv and dz were inverted through Equation A.

Figures 3 and 4 show the map of dv and dz on the whole survey, respectively. The top right corner points to north, which is the shallowest region of the survey, and the bottom left corner points to the south where the water bottom is deeper. In the deeper water bottom area, the maps from either equation were more similar, which was expected.

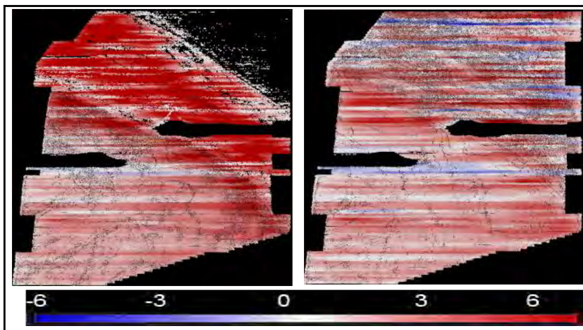

Figure 3: Map of dv. For Equation A (left), the calculated values in the very shallow region are unreliable and discarded, while Equation B (right) provides reasonable values and results in a map that follows the sail line pattern.

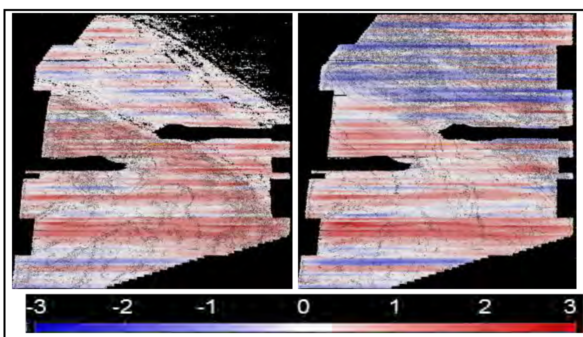

Figure 4: Map of dz for Equation A (left) and Equation B (right). The map from Equation B follows the sailline pattern.

Both methods reduced the normalized root-mean-square (NRMS) value significantly; however, the shallow section regions remained challenging for Equation A, while Equation B provided a better result (Figure 5). The mean NRMS dropped from 51% to 37% using Equation B. This reduction is about 2% lower compared to the reduction with Equation A.

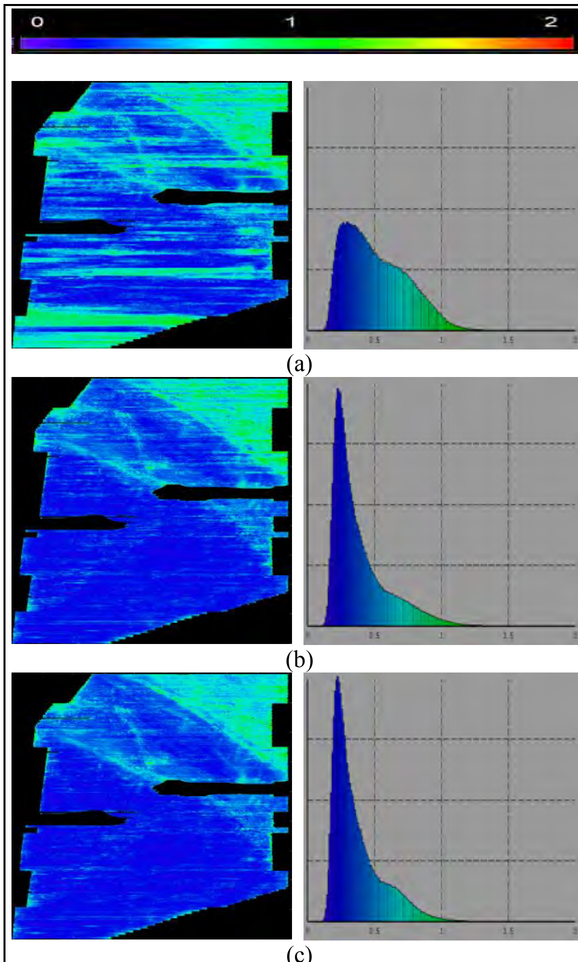

Figure 5: The left column shows the NRMS maps measured in the shallow window where no 4D signal was expected; the corresponding histograms are on the right. (a) Before applying correction. (b) After correction using Equation A. (c) After correction using Equation B.
The stripes on the NRMS map are less evident in (c) compared to (b).

In the 4D stack difference (Figure 6), we did not expect to see 4D signal above the top of reservoir (blue lines). Equation B resulted in the cleanest 4D difference above the reservoir (Figure 6c).

Finally, we examined the timing difference of the stacks between the two vintages. A shallow window was selected to measure the time shift of the two surveys. After applying our method, the timing difference was significantly reduced (Figure 7). Equation B (Figure 7c) had the best result demonstrated by the histogram being more centered at zero and a reduced residual time-shift in the shallow region.

DOI http://dx.doi.org/10.1190/segam2015-5866701.1

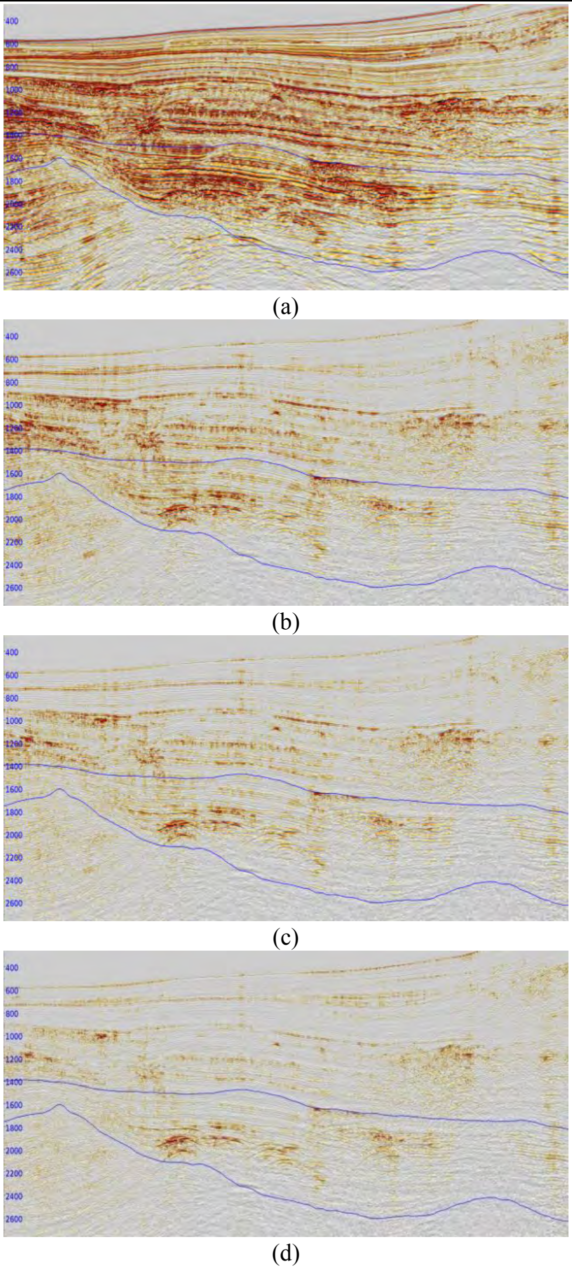

Figure 6: Inline view of 4D stack difference. The blue lines define the reservoir window. (a) Reference stack. (b) Before applying correction. (c) After correction using Equation A. (d) After correction using Equation B.

Conclusion

Our method successfully reduces timing differences between time-lapse data caused by tidal and water velocity differences, which can lead to artificial or inaccurate 4D differences. This method can be applied to both shallow and deep water surveys, and it works well in both sail-line and binned domains.

However, this method only accounts for the 1D effect of water layer variation. If a reflector used is too deep or has a huge dip, the 3D effects are not accounted for in the estimation of dv and dz. Another limitation is that it needs an accurate reference velocity. With a very inaccurate velocity, the events can curve significantly in the far offsets, which lead to an inaccurate time-shift measurement. Consequently, these offsets must be discarded in the estimation. If this leads to too few time-shift and offset pairs, then the data fitting will also be inaccurate and will affect the estimated dv and dz.

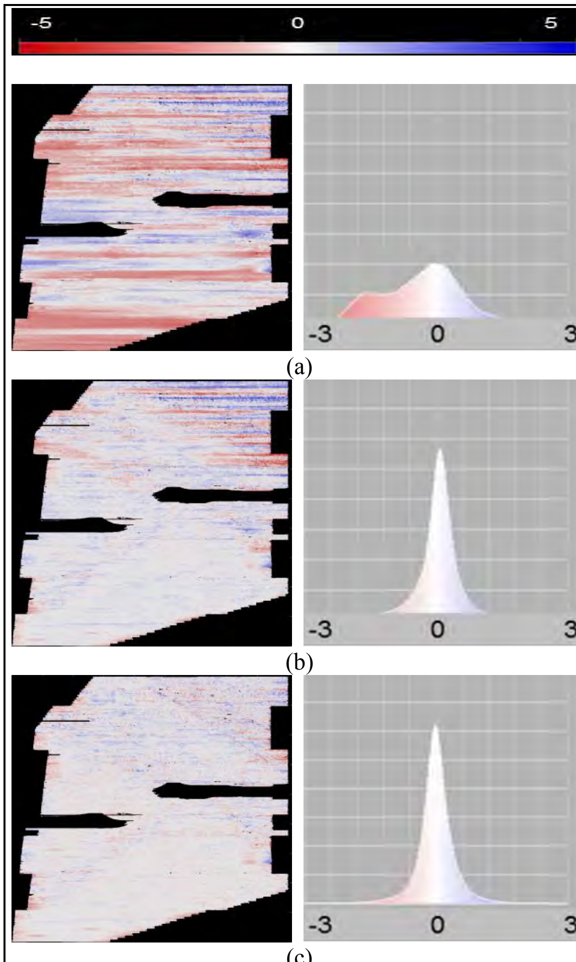

Figure 7: The left column is the time-shift map measured in shallow window; the corresponding histogram is on the right. (a) Before applying correction. (b) After correction using Equation A. (c) After correction using Equation B. Residual time-shift differences remain in the shallow region in (b). The histogram shows that (c) is much more centered at zero.

Acknowledgements

The authors would like to thank CGG for support as well as ExxonMobil Exploration, a division of Exxon Mobil Corporation and Mobil Equatorial Guinea Inc (MEGI) for permission to publish this work. We also thank Yan Huang and Henning Hoeber for helpful discussions and suggestions.

DOI http://dx.doi.org/10.1190/segam2015-5866701.1

EDITED REFERENCES

Note: This reference list is a copyedited version of the reference list submitted by the author. Reference lists for the 2015 SEG Technical Program Expanded Abstracts have been copyedited so that references provided with the online metadata for each paper will achieve a high degree of linking to cited sources that appear on the Web.

REFERENCES

Fried, J., and S. Mackay, 2002, Removing distortions caused by water velocity variations: Water velocity determination: 72nd Annual International Meeting, SEG, Expanded Abstracts, 2070–2073.

Henry, B., S. Butt, M. Igoe, R. Jupp and K. Desrues, 2004, Correction of tidal statics using new generation differential GPS technology: PETEX Conference and Exhibition, Poster Session.

Lacombe, C., J. Schultzen, S. Butt, and D. Lecerf, 2006, Correction for water velocity variations and tidal statics: 68th Conference & Exhibition, EAGE, Extended Abstracts, P098, doi:10.3997/2214-4609.201402385.

Landrø, M., and J. Stammeijer, 2004, Quantitative estimation of compaction and velocity changes using 4D impedance and traveltime changes: Geophysics, **69**, 949–957, http://dx.doi.org/10.1190/1.1778238.